BIOCHEMISTRY
including biophysical chemistry & molecular biology

Article

pubs.acs.org/biochemistry

The TatBC Complex of the Tat Protein Translocase in *Escherichia coli* and Its Transition to the Substrate-Bound TatABC Complex

Jana Behrendt[†,‡] and Thomas Brüser*[,†,‡]

[†]Institute of Microbiology, Leibniz University Hannover, Schneiderberg 50, 30167 Hannover, Germany

[‡]Institute of Biology, Martin Luther University of Halle-Wittenberg, Kurt-Mothes-Strasse 3, 06120 Halle, Germany

ABSTRACT: The twin-arginine translocation (Tat) system serves to transport folded proteins across membranes of prokaryotes and plant plastids. In *Escherichia coli*, a complex consisting of multiple copies of TatB and TatC initiates the transport by binding the signal peptides of the Tat substrates. Using blue-native polyacrylamide gel electrophoresis, bands of TatBC-containing complexes can be detected at molecular masses of 440 and 580 kDa. We systematically analyzed the formation of Tat complexes with TatB or TatC variants that carried point mutations at selected positions. Several mutations resulted in specific disassembly patterns and alterations in the 440 kDa:580 kDa complex ratios. The 440 kDa complex contains only TatBC, whereas the 580 kDa complex consists of TatABC. Substrate binding results in a TatBC−Tat substrate complex at ∼500 kDa and a TatABC−Tat substrate complex at ∼600 kDa. Only the ∼600 kDa complex was detected with nonrecombinant substrate levels and thus could be the physiologically most relevant species. The results suggest that some TatA is usually associated with TatBC, regardless of substrate binding.

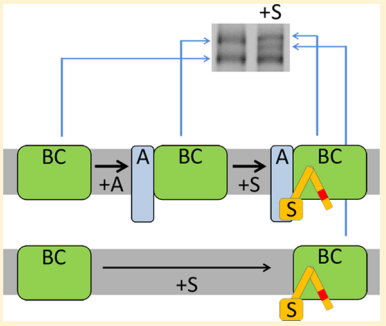

The twin-arginine translocation (Tat) system consists of two membrane-integral complexes that transiently interact to translocate fully folded proteins.[1] In *Escherichia coli* and plant plastids, these complexes are composed of three proteins: TatA forms homooligomers, and TatB tightly associates with TatC. TatBC components recognize the signal peptides of Tat substrates. Thereafter, TatA is recruited and facilitates transport by an unresolved mechanism. TatABC complexes have been found to contain TatB and TatC subunits in a 1:1 ratio, and a variable amount of associated TatA.[2] In bacterial systems, it has not been clarified whether all association of TatA with TatBC depends on substrate binding, but TatA has been proposed to be important for the stability of the TatBC complex.[3] The TatC component contains six transmembrane domains with the N- and C-termini facing the cytoplasm, and it is proposed to form multiple dimers within TatBC complexes.[4] There are natural TatC−TatC tandem fusion proteins in which the two TatC units are separated by two additional transmembrane domains, suggesting close but not direct proximity of the sixth and first transmembrane domains in natural TatC dimers.[5] TatB protomers consist of an N-terminal membrane anchor, directly followed by a hinge region that connects to an amphipathic helix at the inner face of the cytoplasmic membrane and a highly polar region at the C-terminus.[6] Residues in the N-terminal half of TatC most likely play important roles in substrate recognition.[7−12] TatB also takes part in substrate binding, and involved amino acid residues have been genetically identified in the N-terminus.[7,9,13] A direct interaction between TatB and TatC was detected by means of cysteine substitutions positioned at L9 of TatB and M205 of TatC in a transmembrane domain close to the C-terminus of TatC.[14] As TatB binds near the C-terminus of TatC and the substrate interacts with TatB and the N-terminus of TatC, functional TatC is likely to be oligomeric with N- and C-termini of adjacent TatC protomers in the proximity of TatB. A recently determined X-ray structure of *Aquifex aeolicus* TatC protomers and interaction studies with TatC in detergent micelles revealed important interaction sites,[15] but the organization of the oligomeric complexes is still unclear. TatC is able to form a 250 kDa complex in the absence of the other Tat components, which is proposed to form the scaffold for higher-molecular mass TatBC-containing complexes that migrate at apparent masses of 440 and 580 kDa in blue-native polyacrylamide gel electrophoresis (BN-PAGE) analyses.[16,17] Upon membrane solubilization, TatA complexes appear over a broad range of sizes, and it has been proposed that these variable TatA associations could represent gated translocon pores that may have the ability to adjust their diameters to the respective Tat substrate.[18] Alternatively, the "membrane weakening and pulling" model suggests that TatA serves to permeabilize the membrane in the direct vicinity of TatC, while TatC contributes the driving force for unidirectional transport by means of a pulling event.[19] Accumulating evidence favors this model,[20] and molecular dynamics simulations strongly support membrane weakening by TatA.[21]

To gain insights into the formation of TatBC complexes, we analyzed disassembly, TatA association, and substrate binding in more detail. Our data indicate a structural flexibility and modular composition of these assemblies. We could differ-

Received: October 25, 2013
Revised: March 19, 2014
Published: March 21, 2014

   dx.doi.org/10.1021/bi500169s | *Biochemistry* 2014, 53, 2344−2354

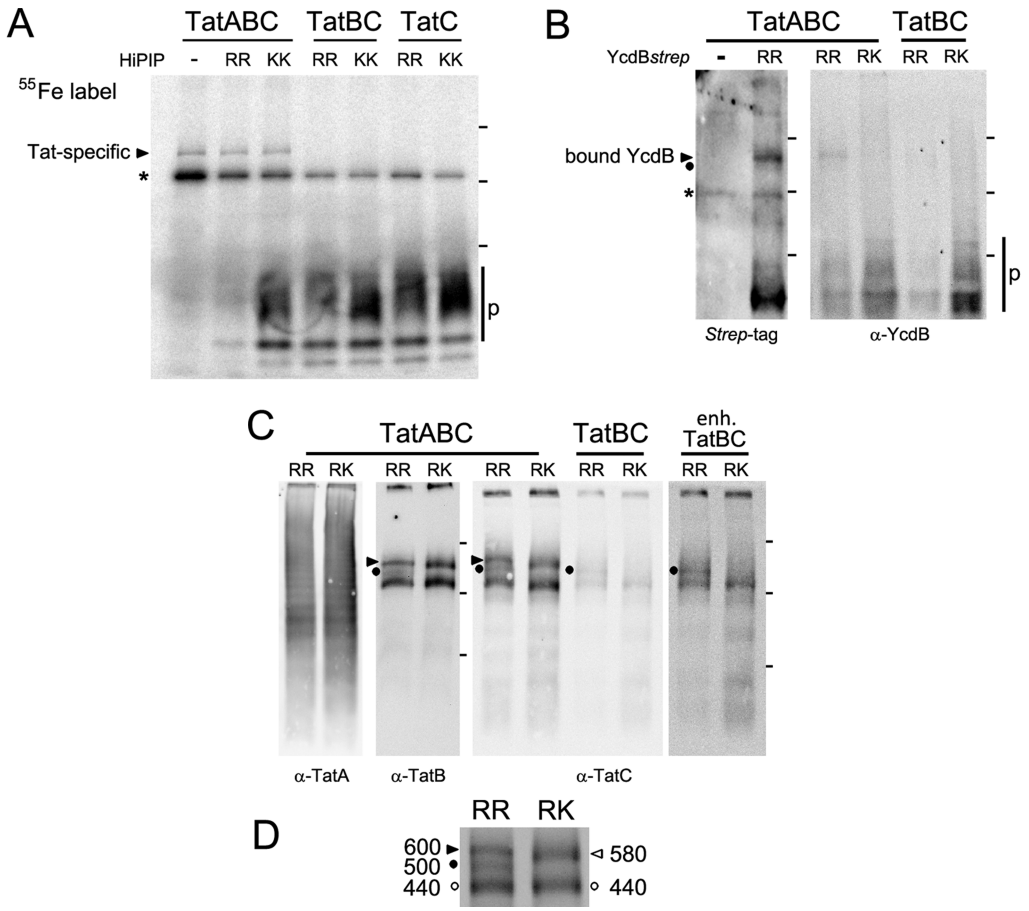

Figure 1. Detection of substrate-bound Tat complexes and requirement of a functional twin-arginine signal peptide for translocon binding. (A) BN-PAGE–autoradiography analysis of ^{55}Fe-labeled proteins in digitonin-solubilized membranes. Strains carrying indicated selected Tat components were generated on the basis of the Tat system deficient strain DADE, using a pABS-*tatABC*, pZA-*tatBC*, or pABS-*tatC* vector for constitutive production of the Tat components. The pZA-*tatBC* vector was designed to achieve fully functional TatBC complexes without excess TatB, which required lower expression levels. Where indicated, the Tat substrate HiPIP with either its natural twin-arginine signal peptide (RR) or the RR>KK mutant derivative (KK) was constitutively produced using the pEXH5-*tac* or pEXH5-KK-*tac* vector, respectively. (B) BN-PAGE–Western blot detection of the twin-arginine-dependent binding of the Tat substrate YcdB in the TatABC- and TatBC-producing strains, using either the *Strep*Tactin–HRP conjugate (left) or YcdB-specific polyclonal antibodies (right). (C) Detection of RR-YcdB-bound complexes (▶ and •) in the presence or absence of TatA. RK-YcdB served as a negative control. Western blot detections of indicated Tat components. An enhanced duplicate of the TatBC lanes demonstrates the presence of the TatBC-dependent 440 and 500 kDa bands and the absence of the 580 and 600 kDa bands in the TatA deficient strain (right, enh. TatBC). (D) TatBC-containing complexes in the 440–600 kDa region as detected by BN-PAGE–Western blot analyses using the TatC antiserum. TatABC strain in combination with RR- or RK-YcdB as used in panel B: (▶) TatABC–Tat substrate complex at ~600 kDa, (•) TatBC–Tat substrate complex at ~500 kDa, (empty triangles and ○) substrate-free 580 kDa TatABC and 440 kDa TatBC complexes, respectively, (*) Tat-unrelated signal, and (p) precursor bands that are not related to TatBC-containing complexes. Positions of marker proteins are indicated (158, 440, and 880 kDa) as small bars on the right sides of the blots.

entiate four distinct high-molecular mass TatBC-containing complexes that differ in TatA and substrate content. Substrate was detected predominantly in TatA-containing complexes.

EXPERIMENTAL PROCEDURES

Strains and Growth Conditions. *E. coli* MC4100[22] or its *tatABCDE* deficient derivative DADE[23] was used for physiological studies, and *E. coli* XL1-Blue Mrf′ Kan (Stratagene) was used for cloning. Strains were grown aerobically at 37 °C in LB medium [1% (w/v) tryptone, 1% (w/v) NaCl, and 0.5% (w/v) yeast extract] in the presence of appropriate antibiotics (100 μg/mL ampicillin and 25 μg/mL chloramphenicol). Cultures were harvested at an OD_{600} of 1.0. Sodium dodecyl sulfate (SDS) sensitivity was determined via aerobic growth in LB medium with or without 4% (w/v) SDS, using the quotient OD_{600} plus SDS/OD_{600} minus SDS after growth for 3 h. Strict TMAO respiratory growth was assessed by growing the strains anaerobically (Hungate tubes) in M9 minimal medium with 0.8% (v/v) glycerol as the sole carbon source, 1.1% (w/v) TMAO, 1 μM Na_2SeO_3, and other trace elements (SL12[24]). Cultures containing pBAD-*ycdB-strep* were harvested after being grown for 2 h with 0.01% arabinose added at an OD_{600} of 0.6. For ^{55}Fe labeling experiments, M9 minimal medium was used and ^{55}Fe (10 μCi) was added to 10 mL growing cultures at an OD_{600} of 0.6. Cells were harvested after growth for an additional hour.

Plasmids and Genetic Methods. The pABS-*tatABC* vector[25] was used for constitutive *tatABC* expression. Single-amino acid exchanges in TatB or TatC were introduced by QuikChange mutagenesis (Stratagene), using the pABS-*tatABC* vector and the following forward primers in conjunction with reverse primers that cover the identical sequence region: *tatB*-D3A-F, GGT GTA ATC CGT GTT TGc cAT CGG TTT

dx.doi.org/10.1021/bi500169s | *Biochemistry* 2014, 53, 2344–2354

TAG CGA AC; *tatB*-E8A-F, GAT ATC GGT TTT AGC Gcc CTG CTA TTG GTG TTC; *tatB*-P22A-F, CGT CGT TCT GGG GgC GCA ACG ACT GCC; *tatB*-K30A-F, GCC TGT GGC GGT Agc cAC GGT AGC GGG CTG; *tatC*-L9A-F, GAA GAT ACT CAA CCG gcc ATC ACG CAT CTG ATT G; *tatC*-R17A-F, CAT CTG ATT GAG CTG gcc AAG CGT CTG CTG AAC TG; *tatC*-P48A-F, CAC CTG GTA TCC GCG gCc TTG ATC AAG CAG TTG; *tatC*-P85A-F, GAT TCT GTC AGC GgC GGT GAT TCT CTA TCA G; *tatC*-F94A-F, CTA TCA GGT GTG GGC Agc gAT CGC CCC AGC GCT G; *tatC*-I95A-F, CAG GTG TGG GCA TTT gcC GCC CCA GCG CTG; *tatC*-P97A-F, GGC ATT TAT CGC CgCcGC GCT GTA TAA GCA TG; *tatC*-E103A-F, CGC TGT ATA AGC ATG cgC GTC GCC TGG TGG TG; *tatC*-E103D-F, CGC TGT ATA AGC ATG AtC GTC GCG TGG TGG TG; *tatC*-F118A-F, CCA GCT CTC TGC TGg ccT ATA TCG GCA TGG C; *tatC*-Y154A-F, CAC CGA CAT CGC CAG Cgc cTT AAG CTT CGT TAT G; *tatC*-P172A-F, GTC TCC TTT GAA GTG gCG GTA GCA ATT GTG C; *tatC*-L189A-F, CCT CGC CAG AAG ACg ccC GCA AAA AAC GCC CG. pBAD-*tatB* and pABS-*tatC* were described previously.[17] The pZA-*tatBC* plasmid was generated by cloning *tatBC* into EcoRI- and PstI-digested pZA31MCS (Expressys) using primers *tatB*-EcoRI-F (GAA GAC GCG AAT TCC CAC GAT AAA GAG C) and *tatC*-PstI-R (GGC GGC TGC AGT TAT TCT TCA GTT TTT TCG). pEXTac-*tatABCstrep* was generated by cloning the *tatABCstrep*-containing NdeI−PvuI fragment from pBW-*tatABCstrep* into the corresponding sites of pEXH5-*tac*.[26] pBW-*tatABCstrep* was generated by cloning a *tatABCstrep* polymerase chain reaction fragment (to fuse a *Strep*-tag II to the C-terminus of TatC) into the NdeI and HindIII sites of pBW22.[27] For pEXTac-*tatABC(E103A)strep*, the E103A exchange was made using the *tatC*-E103A QuikChange primers mentioned above.

For translocation assays, the *hip* gene that encodes the full-length natural HiPIP precursor or the RR>KK variant was co-expressed from the *tac* promoter in pEXH5-*tac* or pEXH5-*tac*-KK, respectively.[26] For YcdB production, the pBAD-*ycdB-strep* vector and a QuikChange-generated derivative encoding RR>RK mutant YcdB (forward primer, *ycdB*-RK-F, GAA CCG TCA CGC AAA CGT TTA CTG AAA) were used.[28] All constructs were confirmed by DNA sequencing.

Biochemical Methods. BN-PAGE was performed with 5 to 13.5% gradient gels, and samples were prepared as described previously,[26] but without β-mercaptoethanol in the buffers. Sodium dodecyl sulfate−polyacrylamide gel electrophoresis (SDS−PAGE) analysis was conducted according to the method of Laemmli,[29] and protein estimations were conducted by the method of Lowry.[30] Subcellular fractionations into the periplasm, membranes, and cytoplasm were performed with 50 mL cultures as described previously.[31] Affinity chromatography was conducted essentially as described previously[2] but with 10% glycerol and 10 mM $MgCl_2$ (no KCl) in all buffers. For immunoblots, proteins were semi-dry-blotted on nitrocellulose membranes, and blots were developed with antibodies directed against synthetic C-terminal peptides of TatA, TatB, TatC, purified HiPIP,[32] or purified YcdB, using the ECL system (GE Healthcare) for signal detection. *Strep* tags were detected by horseradish peroxidase-coupled *Strep*Tactin (IBA). HRP-conjugated goat anti-rabbit antibodies (Bio-Rad) served as secondary antibodies. For stripping, we incubated the blots with 100 mM glycine (pH 2.8), 1% SDS, and 0.2% Tween 20 for 30 min, followed by three washing steps with PBS. This protocol gave no detectable background. The chain formation phenotype was assessed by phase contrast microscopy. Complementation of the SDS sensitivity of the Tat mutant strains was quantified as described by Ize et al.[33]

In the case of ^{55}Fe-containing cells, membranes of 10 mL cell cultures were prepared by lysozyme−osmotic shock treatment of spheroplasts to minimize volumes and contaminations. Spheroplasts, prepared by cold osmotic shock,[31] were resuspended in 0.2 mg/mL lysozyme, 10 mM Tris-HCl (pH 8.0), 0.1 mM EDTA, and 20% sucrose, incubated for 20 min at room temperature, harvested, and again shocked in 5 mM cold $MgSO_4$ to disrupt the cells. After separation of the cell debris, membranes were prepared by ultracentrifugation and used for solubilization and BN-PAGE.

RESULTS

Detection of Iron-Containing Substrates in a Single ~600 kDa TatABC Complex. In BN-PAGE analyses, digitonin-solubilized TatBC-containing complexes migrate at molecular masses of 440 and 580 kDa.[17,26] Multiple TatA signals are detected over a broad range of sizes that correspond to multimeric modular complexes.[34] So far, the question of whether the two TatBC-containing complexes result from differences in subunit composition, complex conformation, or substrate binding could not be answered.[26] To address substrate binding, we added ^{55}Fe to the growth medium, which labels the many Tat substrates that are known to be transported together with assembled iron-containing cofactors[35] (Figure 1A). To look for possible effects of overproduced iron−sulfur cluster-containing Tat substrates, we included recombinant high-potential iron−sulfur protein (HiPIP) and a translocation deficient variant with an RR>KK mutated signal peptide in our analyses.[31] A sharp Tat-specific ^{55}Fe-labeled band at ~600 kDa was detected only when TatA was present in addition to TatB and TatC, which indicates a translocation intermediate after the recruitment of TatA to TatBC [Figure 1A (▶)]. A second, stronger ^{55}Fe signal was diminished in the presence of overproduced HiPIP, irrespective of the presence of RR or KK motifs in the signal peptide [Figure 1A (∗)]. It was also present in Tat deficient membranes and thus unrelated to Tat (data not shown). We suggest that the incorporation of iron into this unknown membrane protein was limited by the reduced availability of free iron due to the excess of heterologous iron-sequestering HiPIP. The TatABC-dependent ^{55}Fe signal at ~600 kDa was largely independent of HiPIP overproduction [Figure 1A (▶)], indicating that the abundance of detected translocation intermediates was not influenced by HiPIP. The easiest explanation for this observation could be a higher affinity of the detected substrates for the Tat translocon and possibly also for iron ions. This higher affinity is likely, as the binding of these Tat substrates to the Tat system resisted detergent treatment, which was not the case for HiPIP.

The Level of Membrane-Associated HiPIP Is Depleted in the Presence of a Functional Tat System. While the HiPIP precursor is only a "weak" translocon-binding substrate that is washed off during solubilization, it is known to interact signal peptide-dependently with biological membranes,[31,36] and this interaction could be nicely detected. The free ^{55}Fe-labeled HiPIP precursor accumulated at the cytoplasmic membrane when transport was compromised by RR>KK mutations or a lack of translocon components [Figure 1A (p)]. Additional diffuse bands indicated multiple interactions with Tat-unrelated

proteins. Importantly, the level of HiPIP in the membrane fraction was depleted when it could be Tat-dependently translocated, i.e., in the presence of the TatABC components and its functional RR signal peptide (Figure 1A, TatABC/RR). This supports the current view that Tat substrates can interact with membranes prior to translocation.[37,38]

YcdB Is Specifically Detected in the ~600 kDa TatABC Complex. As the ^{55}Fe signals indicated iron-containing substrates in ~600 kDa TatABC complexes, we searched for individual Tat substrates that might bind tightly enough to the Tat translocon for detection by immunoblotting. The natural *E. coli* Tat substrate YcdB (also termed EfeB), a heme-containing protein of the DyP peroxidase family involved in iron acquisition,[28,39,40] was detected both by the *Strep*Tactin–HRP conjugate that recognized the C-terminal *Strep* tag of the construct and by a polyclonal YcdB-specific antibody (Figure 1B). In agreement with the ^{55}Fe labeling results, YcdB was found in a Tat-specific complex at ~600 kDa [Figure 1B (▶)]. This band was not detected in the absence of TatA, confirming that the ~600 kDa substrate-containing complex is a TatABC complex (Figure 1B, TatBC). The correlating detections with ^{55}Fe as well as with the YcdB antibody thus both revealed a substrate-containing TatABC complex at ~600 kDa. An RR>RK exchange in the twin-arginine motif virtually abolished the signal, indicating that the interaction depended on the recognition of the RR motif by TatBC. As first observed with the RK variant of the natural Tat substrate GFOR,[41] the RR>RK mutation blocks the transport of YcdB (data not shown). An additional very faint RR-YcdB signal in the region of ~500 kDa [Figure 1B (●)] seemed to be independent of TatA. When we used Tat-specific antibodies to detect TatABC- and TatBC-containing complexes with bound RR-YcdB, using RK-YcdB as negative control, we could differentiate four different high-molecular mass Tat complexes (Figure 1C): the well-known 440 and 580 kDa complexes that were independent of RR-YcdB production and thus likely to be independent of substrate binding (Figure 1C, TatABC RK lanes) and the ~500 and ~600 kDa complexes that were induced by RR-YcdB binding and therefore were the substrate-containing complexes that had been detected in Figure 1B. The 580 and 600 kDa complexes depended on the association of TatA, although the direct detection of TatA as a component of the mentioned Tat complexes was prevented by the many signals of modular TatA complexes in that region (Figure 1C, left panel). The differentiation of all four complexes in BN-PAGE gradient gels is not trivial, especially in the case of the 580 and 600 kDa TatABC complexes that can only be distinguished visually by direct side-by-side comparison. To facilitate further reading, the positions of all Tat complexes in that size range are summarized in Figure 1D. To the best of our knowledge, this is the first detection of a natural Tat substrate bound to a functional bacterial Tat system by BN-PAGE, and the first differentiation of TatA-dependent and -independent TatBC complexes.

Individual Point Mutations in TatB and TatC Affect the BN-PAGE Pattern of TatBC Complexes. We then examined possible effects of single-amino acid substitutions in TatB and TatC subunits to dissect the formation of TatBC-containing complexes in the presence of TatA. Such substitutions were likely to influence detergent resistance and migration behavior of the high-molecular mass Tat complexes in native gels, and we examined a total of 17 point mutations in our screen to find examples that were useful for the identification of assembly intermediates and substrate-bound Tat complexes. Mutations in key regions of TatB included a charge in the extreme N-terminus (D3A), a highly conserved negative charge in the transmembrane region (E8A), an equally conserved proline residue in the hinge region (P22A), and a positive charge in the amphipathic helix (K30A) (Figure 2). For TatC analyses, we selected exchanges at conserved or

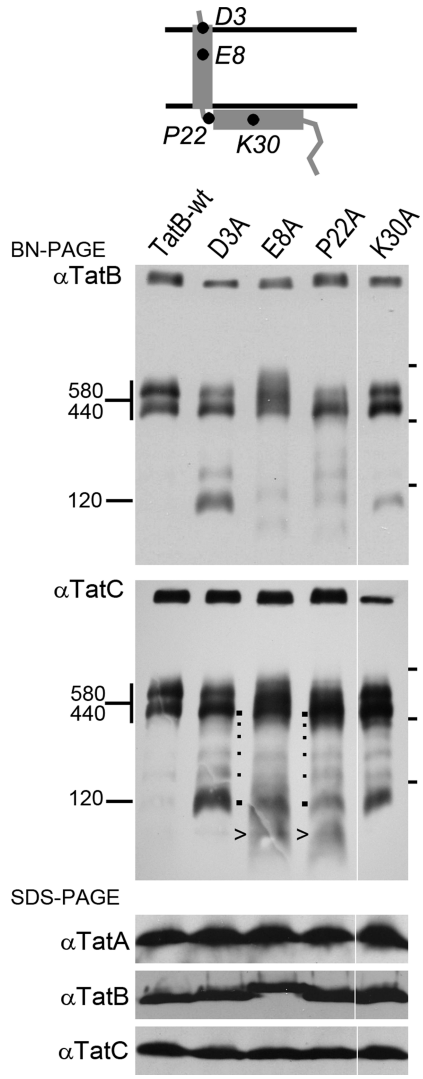

Figure 2. Effect of TatB point mutations on the stability of TatBC complexes. TatBC complexes with the indicated point mutations in TatB were analyzed by BN-PAGE and Western blotting, using antibodies against TatB (top) and TatC (bottom). The positions of the TatB substitutions are schematically depicted above the blots. Mutations were introduced into the low-copy number vector pABS-*tatABC*, which constitutively expresses the *tatABC* operon under control of its natural P_{tatA} promoter. Typical disassembly bands are labeled with dots, with larger dots indicating a pronounced disassembly band at ~120 kDa and the 440 kDa TatBC complex. Positions of the 440 and 580 kDa TatBC complex bands as well as the 120 kDa module are indicated at the left. Arrow heads (>) point to the smallest and more diffuse disassembly product that occurred with TatB-E8A and -P22A mutations. Positions of BN-PAGE marker proteins are indicated as small bars on the right side of the blots (158, 440, and 880 kDa). SDS–PAGE and Western blotting data show that TatABC components were stably produced in comparable amounts (lowermost blots; TatA migrates at 18 kDa, and TatB and TatC migrate near 29 kDa).

dx.doi.org/10.1021/bi500169s | *Biochemistry* 2014, 53, 2344–2354

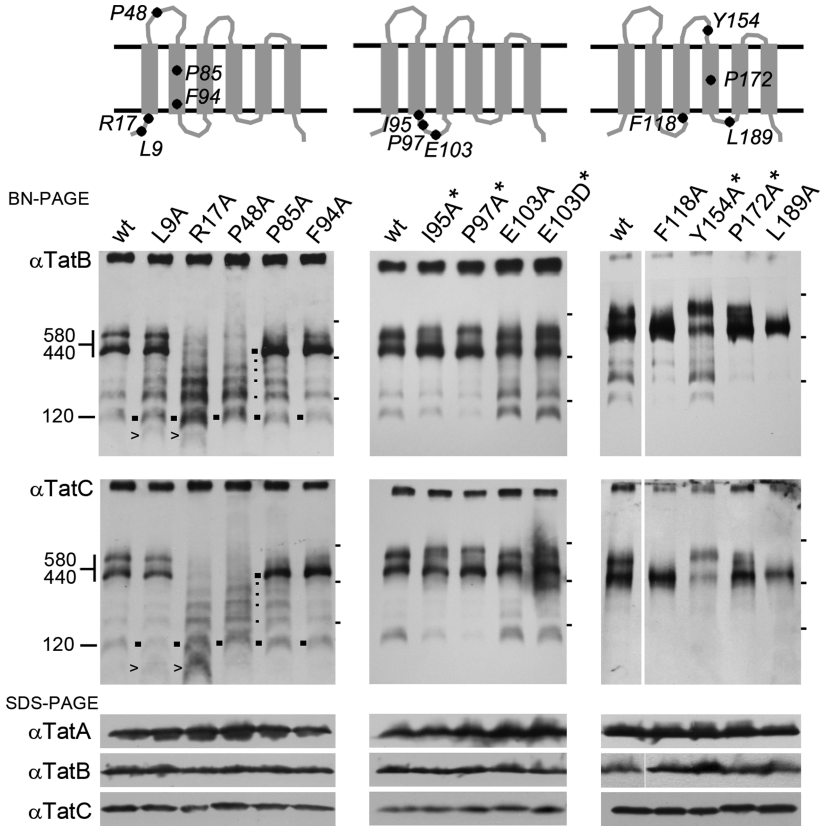

Figure 3. Effect of TatC point mutations on the stability of TatBC complexes. Detection of TatBC-containing complexes as in Figure 2, but with indicated point mutations in TatC. Labels are used as in Figure 2. Arrow heads (>) point to the smallest and more diffuse disassembly product. The asterisks (∗) highlight TatC mutations that result in altered 580 kDa bands. The small bars on the right side of the blots mark positions of BN-PAGE marker proteins (158, 440, and 880 kDa).

experimentally identified important positions (L9A, R17A, P48A, P85A, F94A, I95A, P97A, E103A, E103D, F118A, Y154A, P172A, and L189A) (Figure 3). A control without any point mutation (Figure 2, TatB-wt, and Figure 3, TatC-wt) displayed the typical TatBC complex signals at 440 and 580 kDa.[17,26] Point mutations in TatB and TatC often resulted in the detection of five disassembly bands with both proteins at constant ratios, which suggests a modular assembly of the TatBC complexes [Figures 2 and 3 (■)]. These disassembly patterns slightly varied, but the bottom two disassembly bands were usually most prominent. Clearly, alanine substitutions of TatC-R17 and TatC-P48 strongly affected the assembly of TatBC complexes. These results confirmed earlier analyses of the P48A exchange.[42] Continued dissociation to below 120 kDa was hardly observed, with the exception of TatB-E8A, TatB-P22A, and TatC-R17A mutations. Here, an additional diffuse lower-molecular mass signal corresponds most likely to monomeric TatB and TatC [Figures 2 and 3 (>)]. Therefore, the 120 kDa module could be a minimal TatB- and TatC-containing unit that can oligomerize to form the larger complexes. In previous purification studies, a TatC-His_6-containing complex of similar size was detected.[16] BN-PAGE analyses with the slightly harsher detergent $C_{12}E_9$ in comparison with the more commonly used digitonin revealed the ability of TatB alone to form trimeric modules that can multimerize, whereas the homooligomeric 250 kDa TatC complex consists of six units (Figure 4). Such TatB or TatC self-interactions may trigger the modular assembly to larger TatBC complexes.

Besides the disassembly aspects, we often noted alterations of the 440 kDa:580 kDa band ratios, which were in most cases decreased abundances of the 580 kDa complex that coincided with higher relative abundances of the 440 kDa TatBC complex (Figures 2 and 3). The TatB-E8A and TatB-P22A variants as well as several TatC point mutations (I95A, P97A, E103D, Y154A, and P172A) gave rise to small shifts or doublet signals in the 580 kDa region. F118A and L189A substitutions in TatC resulted in a virtually complete loss of the 580 kDa TatABC complex signal. Only with TatC-Y154A did we observe a depletion of the 440 kDa band, whereas the 580 kDa band was enhanced. In summary, we could successfully identify some TatB and TatC mutations that selectively affected the abundance and pattern of TatBC-containing complexes, which was useful for the envisaged differentiation of the TatABC-dependent 580 and ∼600 kDa complexes.

Effects of Single-Amino Acid Substitutions in TatB and TatC on Activity. Before further analyses, we examined the effects of the mutations on translocation activity. Activity assays that monitor translocation of HiPIP[19] (Figure 5), the TMAO reductase TorA,[43] and amidases AmiA and AmiC[33] (Table 1) by the mutated Tat systems were employed. In agreement with previous studies, HiPIP and TorA transport was completely inhibited by TatC-P48A, TatC-F94A, and TatC-E103A and strongly affected by TatC-E103D.[4,10,12,44,45] The transport of AmiA and AmiC was only abolished by TatC-P48A and TatC-E103A mutations and significantly inhibited by TatC-F94A and TatC-E103D. The strong effects of mutations at positions F94 and E103 most likely relate to substrate

dx.doi.org/10.1021/bi500169s | *Biochemistry* 2014, 53, 2344−2354

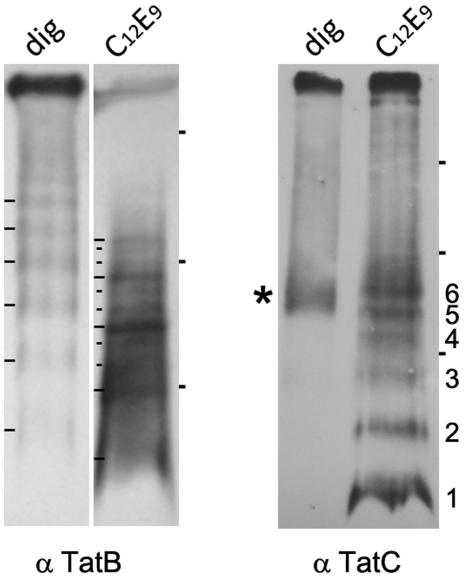

Figure 4. Evidence of trimeric TatB modules and a hexameric 250 kDa TatC complex in the absence of other Tat components. Membranes of strains containing only TatB (DADE pBAD-*tatB*) or only TatC (DADE pABS-*tatC*) have been solubilized by either digitonin (dig) or $C_{12}E_9$ and analyzed by BN-PAGE and Western blotting to detect the respective components. It is known that TatB forms modular "ladders" in the absence of the other Tat components and that TatC forms a 250 kDa complex in BN-PAGE analyses with digitonin as the detergent (left lanes in the two blots and ref 17). Via substitution of digitonin with $C_{12}E_9$ for solubilization, a limited disassembly of the TatB modules and TatC complexes was achieved (right lanes). TatB module bands and intermediate bands that originate from partial disassembly of these modules are indicated by large and small bars, respectively (left panel). The TatC blot shows the 250 kDa TatC complex as seen after digitonin solubilization (∗) and the numbered disassembly bands that are detected after $C_{12}E_9$ solubilization (right panel). Positions of size markers (158, 440, and 880 kDa) are indicated at the right of the blots.

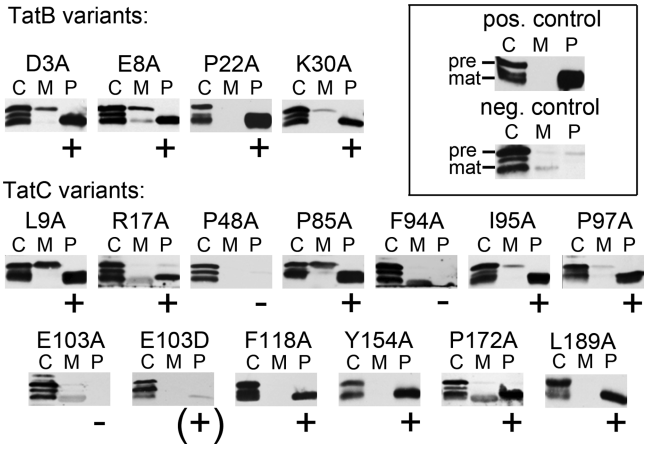

Figure 5. Activity of mutated TatBC complexes. Detection of HiPIP in subcellular fractions of the strains with indicated mutations in TatB or TatC. The Tat substrate HiPIP was constitutively produced using the pEXH5-*tac* vector. Transport is recognized by the presence of mature HiPIP (~12 kDa) in the periplasm, with no significant precursor contamination. Precursor HiPIP (~16 kDa) is exclusively detected in cytoplasm or membrane fractions and is partially degraded to a mature size.

Table 1. TMAO Respiratory Growth, SDS Resistance, and Cell Division Phenotypes of the TatB and TatC Mutated Strains Used in This Study

	TMAO respiration[a]	SDS resistance[b]	chain formation[c]
wt Tat	+++ (1.4 at 21 h)	+++	−
empty vector control	−	−	+
TatB D3A	+++ (1.3 at 27 h)	++	−
TatB E8A	+++ (1.2 at 27 h)	+++	−
TatB P22A	+++ (1.4 at 25 h)	+++	−
TatB K30A	+++ (1.2 at 27 h)	+++	−
TatC L9A	+++ (1.3 at 23 h)	+++	−
TatC R17A	++ (0.8 at 27 h)	+++	−
TatC P48A	−	−	+
TatC P85A	+++ (1.2 at 27 h)	+++	−
TatC F94A	−	+	±
TatC I95A	++ (0.9 at 27 h)	+++	−
TatC P97A	++ (0.75 at 27 h)	+++	−
TatC E103A	−	−	+
TatC E103D	+ (lag of >60 h)	+	+
TatC F118A	+++ (1.4 at 27 h)	+++	−
TatC Y154A	+++ (1.1 at 27 h)	+++	−
TatC P172A	+++ (1.5 at 21 h)	+++	−
TatC L189A	+++ (1.5 at 21 h)	+++	−

[a]TMAO respiratory growth on the nonfermentable carbon source glycerol indicates functional Tat transport of the TMAO reductase TorA: +++, yields similar to those of wild-type Tat systems; ++, small effects on growth; +, strong effects on growth; −, no growth. The maximal OD_{600} and the time point of this maximum are given in parentheses. [b]SDS resistance as monitored by the percentage of liquid culture density (OD_{600}) when cells were grown for 3 h at 4% SDS relative to growth at 0% SDS. Tat deficient strains or strains with nonfunctional Tat systems are highly sensitive to SDS:[33] +++, no significant SDS sensitivity; ++, slight defects in SDS resistance (<80% of that of the wild type); +, strong defects in SDS resistance (<60% of that of the wild type); −, complete SDS sensitivity as found with a Tat deficient strain. [c]Assessment of the cell chain formation phenotype. Cell chains are caused by the impaired translocation of amidases AmiA and AmiC that are involved in cell separation after cell division, which is directly related to the SDS sensitivity phenotype:[33] −, no cell chains formed; ±, short chains of three or four cells; +, long chains of up to 10 cells.

binding,[10] whereas a plausible explanation for the loss of function caused by the P48A exchange in TatC would be the strongly perturbed TatBC assembly process (Table 1 and Figure 3).[42] The TatC-R17A mutation was found to decrease transport activity to a variable extent (Table 1 and Figure 5),[44,45] and our data suggest translocon disassembly as a conceivable reason (Figure 3). TMAO growth data could also reveal minor effects of noninactivating Tat system mutations in the second cytoplasmic TatC domain (I95A, P97A, and F118A) that resulted in retarded growth (Table 1). This underlines the generally accepted importance of this region for substrate binding.[7,10−12]

Mutational Differentiation between the ~600 kDa Substrate-Containing and 580 kDa Substrate-Independent TatABC Complexes. We then analyzed substrate binding effects on mutated Tat complexes with altered migration behavior, namely, TatC-P97A that caused a split 580 kDa signal, TatC-Y154A that depleted the 440 kDa band, TatC-L189A that depleted the 580 kDa complex, and wild-type TatC as a positive control (Figure 6A). The Tat substrate YcdB associated with the wild-type Tat system and with the TatC-

dx.doi.org/10.1021/bi500169s | *Biochemistry* 2014, 53, 2344−2354

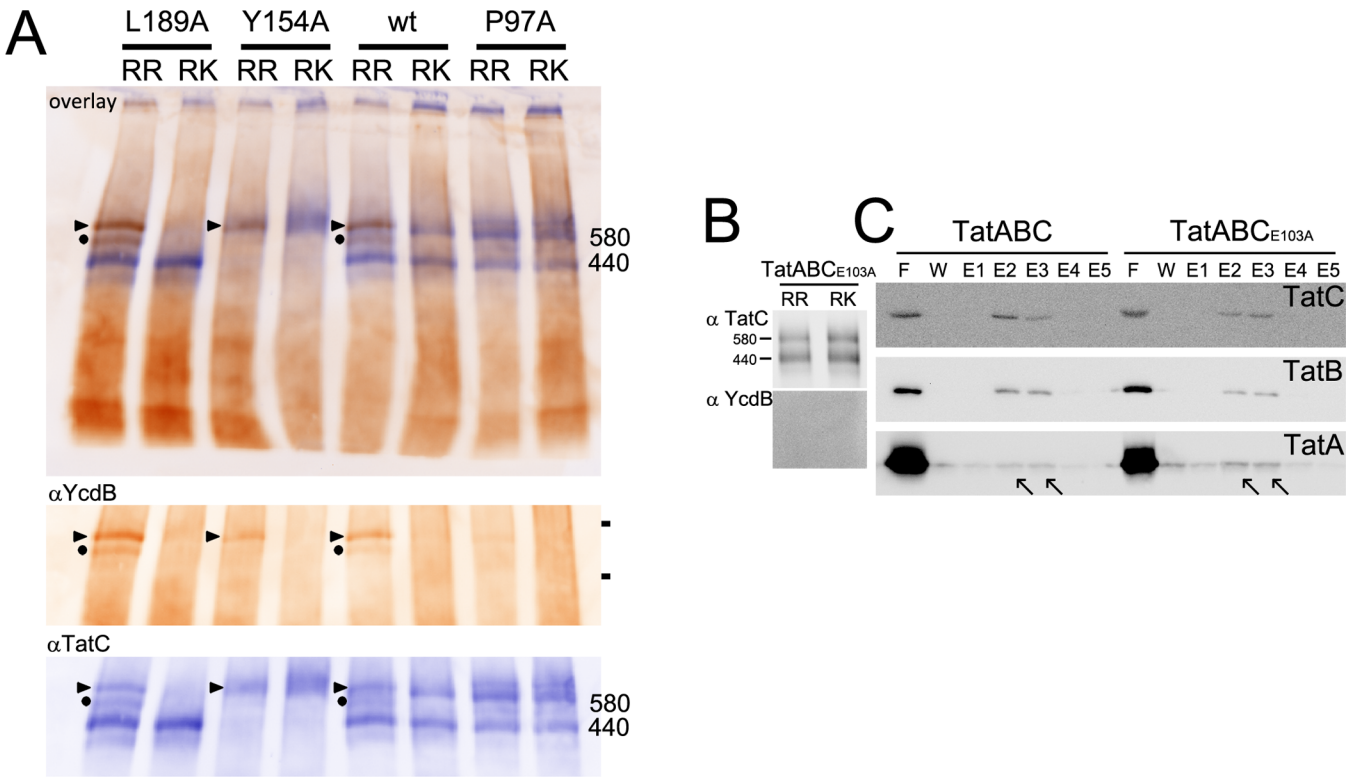

Figure 6. The ~600 kDa translocation intermediate is independent of the relative abundance of 580 kDa complexes and depleted by mutations in the TatC substrate binding site. (A) Substitutions of TatC L189, Y154, and P97 with alanine that caused distinct alterations in the 440 and 580 kDa Tat complex bands (see the text for details) were used to compare substrate-specific signals with individual Tat complex bands. Pseudocolored BN-PAGE–immunoblot detection of TatC (blue) and YcdB (brown) in *E. coli* strain DADE pABS-*tatABC*/pBAD-*ycdB-strep* with the indicated point mutations in TatC or without mutations (wt). The blot was first used to detect YcdB with the YcdB antibody and then stripped and developed with the TatC antibody to localize the TatBC complexes. The top blot shows an overlay that visualizes the position of the YcdB signal relative to the TatBC complexes. Below this overlay, the relevant regions of the YcdB and TatC blots are shown. Positions of the 440 kDa TatBC and 580 kDa TatABC complexes are indicated at the right of the overlay as well as the TatC blot; positions of the RR-YcdB-containing ~600 kDa TatABC (▶) and ~500 kDa TatBC complexes (•) are highlighted on all blots, and positions of marker proteins are given at the right of the YcdB blot (440 and 669 kDa). (B) BN-PAGE analysis as in panel A but with an E103A exchange in TatC. The TatC-E103A mutation completely abolishes substrate binding-induced shifts in the 440–580 kDa region. The top blot is a TatC blot showing the 440 and 580 kDa complexes that are not altered by RR-YcdB overproduction due to the binding site mutation. The bottom blot is a YcdB blot showing that TatC-E103A abolished YcdB binding. (C) Copurification of TatB and TatA with *strep*-tagged TatC as produced from pEXTac-*tatABCstrep* or pEXTac-*tatABC(E103A)strep* in strain DADE, using *Strep*-tactin affinity chromatography followed by SDS–PAGE and Western blotting. Arrows point to co-eluting TatA. Legend: F, flow through; W, last wash fraction; E1–E5, elution fractions.

L189A mutated Tat system in a RR-dependent manner and induced the formation of the substrate-containing ~500 and ~600 kDa bands described above, indicating unaffected substrate binding. However, the TatC L189A mutation selectively affected the 580 kDa TatABC complex without bound substrate, although substrate binding was clearly detected (see Discussion). The TatC-Y154A substitution reduced the detectable YcdB, and the TatC-P97A variant showed an almost complete loss of the YcdB signal. This indicates that YcdB binding is weakened by noninactivating mutations close to the substrate binding site in the first cytoplasmic loop of TatC, which recognizes the RR motif.[46,47] The substrate-bound TatABC complex at ~600 kDa and the weaker ~500 kDa substrate-bound TatBC complex band were clearly detected in these experiments [Figure 6A (▶ and •)]. As seen before, the RR-YcdB signals exactly overlapped with the Tat complex signals (Figure 6A, overlay). A direct comparison of the TatC signals indicated that the relative abundance of 440 or 580 kDa associations was not important for the formation of the substrate-bound complexes (Figure 6A, TatC blot). When these observations are taken into consideration, a possible scenario is that YcdB binding is responsible for the shift of the 440 kDa TatBC and 580 kDa TatABC complexes to ~500 and ~600 kDa, respectively.

Some TatA Is Usually Associated with TatBC, in a Manner Independent of Substrate Binding. Although TatA is required for the formation of the 580 kDa TatABC complex that is independent of substrate binding (Figure 1C, TatABC RK), the direct detection of TatA as a component of this complex by BN-PAGE was not possible because of the aforementioned abundance of modular TatA complexes in that size range. We therefore assessed whether some TatA is associated with TatBC in the absence of substrate by using a TatABC system with a *strep*-tagged TatC-E103A variant. The TatC-E103A mutation abolishes substrate binding and thereby inactivates the Tat system (Table 1 and Figure 6B.C).[10] We confirmed this for the YcdB interaction: no RR-YcdB was bound to Tat complexes with an alanine substitution in TatC-E103, and consequently, neither ~600 nor ~500 kDa Tat-specific complexes were formed (Figure 6B). We then compared copurification of TatA in strains with the wild type or E103A TatC variant (Figure 6C). *strep*-tagged TatC eluted

dx.doi.org/10.1021/bi500169s | *Biochemistry* 2014, 53, 2344–2354

in fractions 2 and 3 from the affinity column, as did TatB, the well-established binding partner of TatC.[2] TatA was continuously washed off (Figure 6C, wash fraction), which indicates an association that is less stable than the TatB−TatC interaction. However, some TatA clearly co-eluted with TatC in fractions E2 and E3, and this co-elution was not abolished by the TatC-E103A mutation that is defective in substrate binding. As the 440 kDa TatBC complex does not require TatA, the detected TatA in copurifications most likely represents subunits of the 580 kDa TatABC complex. These results demonstrate that some TatA is associated with TatBC even when no substrate is bound.

DISCUSSION

Possible Roles of TatA in the Formation of Functional Tat Translocons. We initially suspected that the 580 kDa Tat complex results from binding of the substrate to the 440 kDa TatBC-containing complex.[26] Here we show that it is the binding of TatA that causes this shift, whereas substrate binding triggers the formation of other complexes: an ∼500 kDa TatBC−Tat substrate complex and an ∼600 kDa TatABC−Tat substrate complex. The 580 kDa TatABC complex does not contain substrate and is unaffected by inactivation of the substrate binding site (Figure 6B). In agreement with this finding, we could demonstrate substrate-independent association of TatA with TatBC by copurification (Figure 6C). Most TatBC in the living cell may be organized in such TatABC complexes, although BN-PAGE analyses often predominantly detect the TatBC complex at 440 kDa, possibly as a result of detergent-induced dissociation of more weakly bound TatA. In addition to the TatA subunits that are already associated with TatBC prior to substrate binding, it is known that a significant amount of TatA is transiently recruited after substrate binding to allow translocation.[48,49]

TatABC Complexes Are Not Static: Dynamics in the Tat Translocon. Single-point mutations in TatB or TatC could alter the ratios of 440 kDa TatBC and 580 kDa TatABC complexes, implying that small changes can already (usually negatively) influence the affinity for TatA. The TatA−TatBC interaction thus does not seem to be very robust, and it is possible that TatABC complexes are often not recognized just because of solubilization effects. A second similarly important aspect that arises from the analyses of the mutations is the apparent variability of the 580 kDa complex, including small shifts or double bands (Figures 2 and 3). Knowing that TatA interactions are involved in this complex and knowing that TatBC interactions are quite rigid, we can best explain this variability as differences in the assembly of TatA. As TatA is not associated with the 440 kDa complex, it is not surprising that the point mutations in TatB and TatC do not have any effect on the migration of this complex (Figures 2 and 3). We found that the variability in the 580 kDa band does not correlate with activity defects (Table 1 and Figure 5). Therefore, most likely only assembly states of TatA at TatBC after digitonin solubilization are varying, suggesting that more than one TatA binding site exists at TatBC modules and mutations affect individual binding sites without abolishing overall TatA recruitment or transport function.

Tat Substrates Bind to High-Molecular Mass Tat Complexes in *E. coli* Membranes. As mentioned above, substrate recruitment results in ∼500 and ∼600 kDa Tat complexes. In our substrate binding analyses, the ∼600 kDa TatABC complex was the predominant substrate-containing complex and it is possible that the 580 kDa complex represents its corresponding substrate-free form, because both complexes require TatA for assembly (Figures 1 and 6). In BN-PAGE, the 580 and ∼600 kDa TatABC complexes migrate very close and can be differentiated only by direct side-by-side comparisons. Their clear distinction was achieved by the use of mutated Tat systems. (i) The 580 kDa band is not depleted by the TatC-P97A mutation that renders the substrate binding site detergent sensitive (Figure 6A) or by the TatC-E103A mutation that completely abolishes substrate binding (Figures 2 and 6B). (ii) The TatC-L189A mutation results in the virtual absence of the 580 kDa band without affecting the ∼600 kDa substrate-containing complex (Figure 6A). (iii) The TatC-Y154A mutation causes a depletion of the 440 kDa signal and a shift to the 580 kDa band, although this substitution weakens Tat substrate binding (Figures 2 and 6A). It is surprising that point mutations that alter the migration behavior and abundance of the 580 kDa complex do not influence the appearance of the ∼600 kDa substrate-bound TatABC complex. Especially the TatC-L189A mutation, which diminishes the 580 kDa TatABC complex to a great extent, does not affect the substrate-bound ∼600 kDa complex. We conclude that either the two TatA-containing complexes are independently formed or substrate binding in the ∼600 kDa complex causes an apparently more stable structure. Other published studies, especially those of the plant Tat systems, also suggest that large Tat complexes bind substrates. The TatBC complexes in pea thylakoids migrate as single or double bands between 440 and 880 kDa marker proteins in BN-PAGE analyses, very similar to *E. coli* TatBC.[11,50−52] Accordingly, substrate was detected in one or two bands in this size range.[50−53] As in our experiments, four TatBC complexes have been identified in *Arabidopsis thaliana* (at 310, 370, 560, and 620 kDa), with substrate binding activity attributed to the 560 and 620 kDa species.[54] Certainly, the migration behavior of protein complexes in BN-PAGE gradient gels can differ between organisms, and it might also well be that the detected Tat complexes represent only a detergent-resistant core of an even larger association; however, the similarities strongly suggest that a substrate-containing large TatABC complex is a general intermediate of Tat transport.

Because of the transient nature of the functional substrate-bound Tat complex, only the substrate-free 440 and 580 kDa associations are usually seen in BN-PAGE analyses with recombinant as well as nonrecombinant systems (Figures 2 and 3).[26,55] By using radioactive ^{55}Fe labeling that allows highly sensitive detection, the ∼600 kDa TatABC complex was the only substrate-containing complex at nonrecombinant substrate levels (Figure 1A, lane −). Even though ^{55}Fe likely labels a multitude of Tat substrates of different sizes, we detected only this single band. In line with this, the same ∼600 kDa signal was observed with recombinant RR-YcdB (Figures 1B and 6A) or with recombinant RR-PhoA.[26] We also did not obtain evidence of additional signals that could be due to more than one bound substrate. Although we certainly cannot completely exclude the possibility that the resolution of BN-PAGE was insufficient to reveal effects of different sizes or numbers of substrates, these data suggest that the Tat substrates are buried within Tat complex micelles, thereby hardly influencing the overall shape or dimensions that are responsible for the BN-PAGE migration behavior. A single band of the substrate-containing TatABC complex is suggestive for a recruitment of a constant number of TatA protomers in the TatABC core. This idea is in line with TatA assembly studies in the plant Tat

system, which showed that signal peptides alone can induce a similar TatA oligomerization as do full-length Tat substrates.[49] In addition to the TatA that is part of a core TatABC complex, further TatA is transiently recruited for the translocation event, which has been demonstrated by cross-linking analyses.[51] The amount of TatA in thylakoids is adjusted to a specific level for efficient translocation.[56]

Modular Assembly of TatBC-Containing Complexes. The Tat translocon consists of multiple subunits, and the extent to which oligomerization is required for activity is a central question in the field. Detergent solubilization of *Aquifex aeolicus* TatC resulted in dimers that were not preserved in crystals of these preparations.[15,57] A dimer has been modeled *in silico*, but a substrate binding model was based on a single TatC.[57] The question of whether TatC acts as a monomer even though it assembles as large complexes arises. Our data obtained with mutations that trigger dissociation of Tat components suggest that the complexes are assemblies of TatBC modules (Figures 2 and 3, 120 kDa band). Such modules could be based on a TatC dimer, which is supported by several observations. (i) The detergent-solubilized TatC that had been used for crystallization was dimeric in solution and capable of substrate binding.[15] (ii) Natural dimers of TatC exist in some archaea.[5] (iii) Experiments with functional tandem fusions of TatC also support dimer formation.[4] TatB may help to connect TatBC modules and has been shown to promote the formation of larger complexes.[17] TatB alone as well as TatC alone can self-interact to form trimers or hexamers, respectively, and these interactions may well play a role in the assembly pathway (Figure 4). The interaction of TatB with TatC is highly important for the formation of the substrate binding site[7] and influences the signal peptide insertase activity of TatC, which is likely to be of key importance for the transport mechanism.[58] As the functionally important TatB−TatC interaction is also the basis for the formation of the large TatBC complexes, it is not surprising that bound substrates could be detected only in such large complexes and not in disassembly products (Figures 1 and 6). With nonrecombinant substrate levels, substrates were detected only in the ∼600 kDa TatABC−Tat substrate complex (Figure 1A). The physiological Tat translocon with high affinity for Tat substrates is therefore a large TatABC complex, and the affinity for substrates is most likely markedly decreased when solubilization results in disassembly. The disassembly may be one reason for the difference of several orders of magnitude between substrate affinities of native TatABC-containing membranes[59] and solubilized Tat systems.[15]

AUTHOR INFORMATION

Corresponding Author

*Telephone: +49 511 762 5945. Fax: +49 511 762 5287. E-mail: brueser@ifmb.uni-hannover.de.

Funding

This work was funded by the Deutsche Forschungsgemeinschaft (DFG, GRK 1026 "Conformational transitions in macromolecular interactions").

Notes

The authors declare no competing financial interest.

ACKNOWLEDGMENTS

We thank Sybille Traupe for excellent technical support and Eyleen Heidrich for donating vectors.

ABBREVIATIONS

AmiA and AmiC, murine amidases; BN-PAGE, blue-native polyacrylamide gel electrophoresis; $C_{12}E_9$, dodecylnonaethylene glycol ether; DyP, dye decolorizing peroxidase; EDTA, ethylenediaminetetraacetic acid; HiPIP, high-potential iron−sulfur protein; HRP, horseradish peroxidase; PBS, phosphate-buffered saline; PhoA, alkaline phosphatase; SDS, sodium dodecyl sulfate; SDS−PAGE, sodium dodecyl sulfate−polyacrylamide gel electrophoresis; Tat, twin-arginine translocation; TMAO, trimethylamine *N*-oxide; TorA, TMAO reductase; YcdB, Tat-dependently translocated peroxidase.

REFERENCES

(1) Palmer, T., and Berks, B. C. (2012) The twin-arginine translocation (Tat) protein export pathway. *Nat. Rev. Microbiol. 10*, 483−496.

(2) Bolhuis, A., Mathers, J. E., Thomas, J. D., Barrett, C. M., and Robinson, C. (2001) TatB and TatC form a functional and structural unit of the twin-arginine translocase from *Escherichia coli*. *J. Biol. Chem. 276*, 20213−20219.

(3) Mangels, D., Mathers, J., Bolhuis, A., and Robinson, C. (2005) The core TatABC complex of the twin-arginine translocase in *Escherichia coli*: TatC drives assembly whereas TatA is essential for stability. *J. Mol. Biol. 345*, 415−423.

(4) Maldonado, B., Buchanan, G., Müller, M., Berks, B. C., and Palmer, T. (2011) Genetic evidence for a TatC dimer at the core of the *Escherichia coli* twin arginine (Tat) protein translocase. *J. Mol. Microbiol. Biotechnol. 20*, 168−175.

(5) Dilks, K., Gimenez, M. I., and Pohlschröder, M. (2005) Genetic and biochemical analysis of the twin-arginine translocation pathway in halophilic archaea. *J. Bacteriol. 187*, 8104−8113.

(6) Koch, S., Fritsch, M. J., Buchanan, G., and Palmer, T. (2012) *Escherichia coli* TatA and TatB proteins have N-out, C-in topology in intact cells. *J. Biol. Chem. 287*, 14420−14431.

(7) Lausberg, F., Fleckenstein, S., Kreutzenbeck, P., Fröbel, J., Rose, P., Müller, M., and Freudl, R. (2012) Genetic evidence for a tight cooperation of TatB and TatC during productive recognition of twin-arginine (Tat) signal peptides in *Escherichia coli*. *PLoS One 7*, e39867.

(8) Strauch, E. M., and Georgiou, G. (2007) *Escherichia coli tatC* mutations that suppress defective twin-arginine transporter signal peptides. *J. Mol. Biol. 374*, 283−291.

(9) Kreutzenbeck, P., Kröger, C., Lausberg, F., Blaudeck, N., Sprenger, G. A., and Freudl, R. (2007) *Escherichia coli* twin arginine (Tat) mutant translocases possessing relaxed signal peptide recognition specificities. *J. Biol. Chem. 282*, 7903−7911.

(10) Holzapfel, E., Eisner, G., Alami, M., Barrett, C. M., Buchanan, G., Lüke, I., Betton, J. M., Robinson, C., Palmer, T., Moser, M., and Müller, M. (2007) The entire N-terminal half of TatC is involved in twin-arginine precursor binding. *Biochemistry 46*, 2892−2898.

(11) Ma, X., and Cline, K. (2013) Mapping the signal peptide binding and oligomer contact sites of the core subunit of the pea twin arginine protein translocase. *Plant Cell 25*, 999−1015.

(12) Zoufaly, S., Fröbel, J., Rose, P., Flecken, T., Maurer, C., Moser, M., and Müller, M. (2012) Mapping precursor-binding site on TatC subunit of twin arginine-specific protein translocase by site-specific photo cross-linking. *J. Biol. Chem. 287*, 13430−13441.

(13) Maurer, C., Panahandeh, S., Jungkamp, A. C., Moser, M., and Müller, M. (2010) TatB functions as an oligomeric binding site for folded Tat precursor proteins. *Mol. Biol. Cell 21*, 4151−4161.

(14) Kneuper, H., Maldonado, B., Jäger, F., Krehenbrink, M., Buchanan, G., Keller, R., Müller, M., Berks, B. C., and Palmer, T. (2012) Molecular dissection of TatC defines critical regions essential for protein transport and a TatB-TatC contact site. *Mol. Microbiol. 85*, 945−961.

(15) Rollauer, S. E., Tarry, M. J., Graham, J. E., Jaaskelainen, M., Jäger, F., Johnson, S., Krehenbrink, M., Liu, S. M., Lukey, M. J., Marcoux, J., McDowell, M. A., Rodriguez, F., Roversi, P., Stansfeld, P.

J., Robinson, C. V., Sansom, M. S., Palmer, T., Hogbom, M., Berks, B. C., and Lea, S. M. (2012) Structure of the TatC core of the twin-arginine protein transport system. *Nature 492*, 210−214.
(16) Orriss, G. L., Tarry, M. J., Ize, B., Sargent, F., Lea, S. M., Palmer, T., and Berks, B. C. (2007) TatBC, TatB, and TatC form structurally autonomous units within the twin arginine protein transport system of *Escherichia coli*. *FEBS Lett. 581*, 4091−4097.
(17) Behrendt, J., Lindenstrauß, U., and Brüser, T. (2007) The TatBC complex formation suppresses a modular TatB-multimerization in *Escherichia coli*. *FEBS Lett. 581*, 4085−4090.
(18) Gohlke, U., Pullan, L., McDevitt, C. A., Porcelli, I., de Leeuw, E., Palmer, T., Saibil, H. R., and Berks, B. C. (2005) The TatA component of the twin-arginine protein transport system forms channel complexes of variable diameter. *Proc. Natl. Acad. Sci. U.S.A. 102*, 10482−10486.
(19) Brüser, T., and Sanders, C. (2003) An alternative model of the twin arginine translocation system. *Microbiol. Res. 158*, 7−17.
(20) Hou, B., and Brüser, T. (2011) The Tat-dependent protein translocation pathway. *Biomol. Concepts 2*, 507−523.
(21) Rodriguez, F., Rouse, S. L., Tait, C. E., Harmer, J., De Riso, A., Timmel, C. R., Sansom, M. S., Berks, B. C., and Schnell, J. R. (2013) Structural model for the protein-translocating element of the twin-arginine transport system. *Proc. Natl. Acad. Sci. U.S.A. 110*, E1092−E1101.
(22) Casadaban, M. J. (1976) Transposition and fusion of the lac genes to selected promoters in *Escherichia coli* using bacteriophage lambda and Mu. *J. Mol. Biol. 104*, 541−555.
(23) Wexler, M., Sargent, F., Jack, R. L., Stanley, N. R., Bogsch, E. G., Robinson, C., Berks, B. C., and Palmer, T. (2000) TatD is a cytoplasmic protein with DNase activity. No requirement for TatD family proteins in sec-independent protein export. *J. Biol. Chem. 275*, 16717−16722.
(24) Overmann, J., Fischer, U., and Pfennig, N. (1992) A new purple sulfur bacterium from saline littoral sediments *Thiorhodovibrio winogradskyi* gen. nov. and sp. nov. *Arch. Microbiol. 157*, 329−335.
(25) Berthelmann, F., and Brüser, T. (2004) Localization of the Tat translocon components in *Escherichia coli*. *FEBS Lett. 569*, 82−88.
(26) Richter, S., and Brüser, T. (2005) Targeting of unfolded PhoA to the TAT translocon of *Escherichia coli*. *J. Biol. Chem. 280*, 42723−42730.
(27) Wilms, B., Hauck, A., Reuss, M., Syldatk, C., Mattes, R., Siemann, M., and Altenbuchner, J. (2001) High-cell-density fermentation for production of L-N-carbamoylase using an expression system based on the *Escherichia coli rhaBAD* promoter. *Biotechnol. Bioeng. 73*, 95−103.
(28) Sturm, A., Schierhorn, A., Lindenstrauss, U., Lilie, H., and Brüser, T. (2006) YcdB from *Escherichia coli* reveals a novel class of Tat-dependently translocated hemoproteins. *J. Biol. Chem. 281*, 13972−13978.
(29) Laemmli, U. K. (1970) Cleavage of structural proteins during the assembly of the head of bacteriophage T4. *Nature 227*, 680−685.
(30) Lowry, O. H., Rosebrough, N. J., Farr, A. L., and Randall, R. J. (1951) Protein measurement with the Folin phenol reagent. *J. Biol. Chem. 193*, 265−275.
(31) Brüser, T., Yano, T., Brune, D. C., and Daldal, F. (2003) Membrane targeting of a folded and cofactor-containing protein. *Eur. J. Biochem. 270*, 1211−1221.
(32) Brüser, T., Deutzmann, R., and Dahl, C. (1998) Evidence against the double-arginine motif as the only determinant for protein translocation by a novel Sec-independent pathway in *Escherichia coli*. *FEMS Microbiol. Lett. 164*, 329−336.
(33) Ize, B., Stanley, N. R., Buchanan, G., and Palmer, T. (2003) Role of the *Escherichia coli* Tat pathway in outer membrane integrity. *Mol. Microbiol. 48*, 1183−1193.
(34) Oates, J., Barrett, C. M., Barnett, J. P., Byrne, K. G., Bolhuis, A., and Robinson, C. (2005) The *Escherichia coli* twin-arginine translocation apparatus incorporates a distinct form of TatABC complex, spectrum of modular TatA complexes and minor TatAB complex. *J. Mol. Biol. 346*, 295−305.
(35) Berks, B. C., Palmer, T., and Sargent, F. (2005) Protein targeting by the bacterial twin-arginine translocation (Tat) pathway. *Curr. Opin. Microbiol. 8*, 174−181.
(36) Brehmer, T., Kerth, A., Graubner, W., Malesevic, M., Hou, B., Brüser, T., and Blume, A. (2012) Negatively charged phospholipids trigger the interaction of a bacterial Tat substrate precursor protein with lipid monolayers. *Langmuir 28*, 3534−3541.
(37) Bageshwar, U. K., Whitaker, N., Liang, F. C., and Musser, S. M. (2009) Interconvertibility of lipid- and translocon-bound forms of the bacterial Tat precursor pre-SufI. *Mol. Microbiol. 74*, 209−226.
(38) Hou, B., Frielingsdorf, S., and Klösgen, R. B. (2006) Unassisted membrane insertion as the initial step in ΔpH/Tat-dependent protein transport. *J. Mol. Biol. 355*, 957−967.
(39) Cao, J., Woodhall, M. R., Alvarez, J., Cartron, M. L., and Andrews, S. C. (2007) EfeUOB (YcdNOB) is a tripartite, acid-induced and CpxAR-regulated, low-pH Fe^{2+} transporter that is cryptic in *Escherichia coli* K-12 but functional in *E. coli* O157:H7. *Mol. Microbiol. 65*, 857−875.
(40) Miethke, M., Monteferrante, C. G., Marahiel, M. A., and van Dijl, J. M. (2013) The *Bacillus subtilis* EfeUOB transporter is essential for high-affinity acquisition of ferrous and ferric iron. *Biochim. Biophys. Acta 1833*, 2267−2278.
(41) Halbig, D., Wiegert, T., Blaudeck, N., Freudl, R., and Sprenger, G. A. (1999) The efficient export of NADP-containing glucose-fructose oxidoreductase to the periplasm of *Zymomonas mobilis* depends both on an intact twin-arginine motif in the signal peptide and on the generation of a structural export signal induced by cofactor binding. *Eur. J. Biochem. 263*, 543−551.
(42) Barrett, C. M., Mangels, D., and Robinson, C. (2005) Mutations in subunits of the *Escherichia coli* twin-arginine translocase block function via differing effects on translocation activity or Tat complex structure. *J. Mol. Biol. 347*, 453−463.
(43) Bogsch, E. G., Sargent, F., Stanley, N. R., Berks, B. C., Robinson, C., and Palmer, T. (1998) An essential component of a novel bacterial protein export system with homologues in plastids and mitochondria. *J. Biol. Chem. 273*, 18003−18006.
(44) Buchanan, G., de Leeuw, E., Stanley, N. R., Wexler, M., Berks, B. C., Sargent, F., and Palmer, T. (2002) Functional complexity of the twin-arginine translocase TatC component revealed by site-directed mutagenesis. *Mol. Microbiol. 43*, 1457−1470.
(45) Allen, S. C., Barrett, C. M., Ray, N., and Robinson, C. (2002) Essential cytoplasmic domains in the *Escherichia coli* TatC protein. *J. Biol. Chem. 277*, 10362−10366.
(46) Gerard, F., and Cline, K. (2006) Efficient twin arginine translocation (Tat) pathway transport of a precursor protein covalently anchored to its initial cpTatC binding site. *J. Biol. Chem. 281*, 6130−6135.
(47) Alami, M., Lüke, I., Deitermann, S., Eisner, G., Koch, H. G., Brunner, J., and Müller, M. (2003) Differential interactions between a twin-arginine signal peptide and its translocase in *Escherichia coli*. *Mol. Cell 12*, 937−946.
(48) Dabney-Smith, C., and Cline, K. (2009) Clustering of C-Terminal Stromal Domains of Tha4 Homo-Oligomers during Translocation by the Tat Protein Transport System. *Mol. Biol. Cell 20*, 2060−2069.
(49) Dabney-Smith, C., Mori, H., and Cline, K. (2006) Oligomers of Tha4 organize at the thylakoid Tat translocase during protein transport. *J. Biol. Chem. 281*, 5476−5483.
(50) Berghöfer, J., and Klösgen, R. B. (1999) Two distinct translocation intermediates can be distinguished during protein transport by the TAT (Δph) pathway across the thylakoid membrane. *FEBS Lett. 460*, 328−332.
(51) Cline, K., and Mori, H. (2001) Thylakoid ΔpH-dependent precursor proteins bind to a cpTatC-Hcf106 complex before Tha4-dependent transport. *J. Cell Biol. 154*, 719−729.
(52) Pal, D., Fite, K., and Dabney-Smith, C. (2013) Direct interaction between a precursor mature domain and transport component Tha4 during twin arginine transport of chloroplasts. *Plant Physiol. 161*, 990−1001.

(53) Frielingsdorf, S., and Klösgen, R. B. (2007) Prerequisites for terminal processing of thylakoidal Tat substrates. *J. Biol. Chem. 282*, 24455−24462.
(54) Jakob, M., Kaiser, S., Gutensohn, M., Hanner, P., and Klösgen, R. B. (2009) Tat subunit stoichiometry in *Arabidopsis thaliana* challenges the proposed function of TatA as the translocation pore. *Biochim. Biophys. Acta 1793*, 388−394.
(55) Barrett, C. M., Freudl, R., and Robinson, C. (2007) Twin arginine translocation (Tat)-dependent export in the apparent absence of TatABC or TatA complexes using modified *Escherichia coli* TatA subunits that substitute for TatB. *J. Biol. Chem. 282*, 36206−36213.
(56) Hauer, R. S., Schlesier, R., Heilmann, K., Dittmar, J., Jakob, M., and Klösgen, R. B. (2013) Enough is enough: TatA demand during Tat-dependent protein transport. *Biochim. Biophys. Acta 1833*, 957−965.
(57) Ramasamy, S., Abrol, R., Suloway, C. J., and Clemons, W. M., Jr. (2013) The Glove-like Structure of the Conserved Membrane Protein TatC Provides Insight into Signal Sequence Recognition in Twin-Arginine Translocation. *Structure 21*, 777−788.
(58) Fröbel, J., Rose, P., Lausberg, F., Blummel, A. S., Freudl, R., and Müller, M. (2012) Transmembrane insertion of twin-arginine signal peptides is driven by TatC and regulated by TatB. *Nat. Commun. 3*, 1311.
(59) Whitaker, N., Bageshwar, U. K., and Musser, S. M. (2012) Kinetics of precursor interactions with the bacterial Tat translocase detected by real-time FRET. *J. Biol. Chem. 287*, 11252−11260.